Hindawi
Mobile Information Systems
Volume 2022, Article ID 5620287, 7 pages
https://doi.org/10.1155/2022/5620287

Research Article

Sports Image Decomposition Strategy Based on Moreau Envelope and Depth Recovery

Li Qiang

College of Physical Education, Shaanxi XueQian Normal University, Xi'an, Shaanxi, China 710100

Correspondence should be addressed to Li Qiang; 54025@snsy.edu.cn

Received 21 March 2022; Revised 1 April 2022; Accepted 11 April 2022; Published 10 June 2022

Academic Editor: M. Praveen Kumar Reddy

Sports image decomposition technology is utilized broadly in different fields, and the technologies of sports image action identification situated on sports picture transformation technologies may be suitable. This paper utilizes the Moreau envelope and depth recovery for sports image decomposition strategy, an order of work such as a collection of sports image characteristic distillation, and action identification must be achieved in beginning and started with texture functions as well as various relevant functions. And both algorithms have to be utilized to finish the sports picture-oriented sports action identification technology at the lowest time expense. For the improvement of the latest sports image industry form, which is also strongly developed, the people's affection for sports image is gaining as powerful and creates an improvement of sports image industry still achieving a lot of advantages. The parameters recognition rate and accuracy are compared with various techniques. The proposed methods are effective to achieve the perfect sports image decomposition.

1. Introduction

The concept of a Moreau envelope is a midpoint to the analysis of first-order growth algorithms for machine education [1]. It has not been grown yet and is being lengthened to be utilised on a broad network and, more deeply, as a machine education system with various programming utilizations. The structural arithmetic for Moreau envelopes that has been demonstrated, as well as how to incorporate them into various computer languages, are explained. The invented framework casts in a mathematical growth framework various developed forms of gradient back-propagation connected to the concept of the propagation of essential goals [2]. The Moreau envelope is a path to soft and unique convex performance such that its slope can be computed given the near of the original. The recent performance has the alike critical points as the original. It is also known as the Moreau-Yosida regularization [3]. Decomposing a sports picture into significant elements is considered an essential as well as difficult opposite issue in image transformation. Denoising models are the first range: In those designs, the picture is pretended to have been destroyed by sound, and the transformation aim is ignoring the sound. This thing has to be considered a transformation of the picture into the signal section as well as the noise section. Some presumptions are captured, according to the noise as well as signal, like the piecewise soft originality of the picture, which allows well approximations of the perfect original picture. In recent picture transformation, two major ways are regarded to clear up the denoising issue. The first thing is dependent on handling physically the wavelet coefficients of the picture The next thing is depending on clearing nonlinear partial-differential equations related to the belittlement of energy composed of a few rules of the slope [4].

The concept of morphologically decomposing a signal into its construction blocks is an essential issue in signal transformation and has widespread uses in science and technology [5]. Pentland expressed an algorithm in 1987 for sensing scene depth by calibrating the amount of defocus of an image. The algorithm is interesting in the sensation that no correspondence issues are included [6]. The depth recovery work is to recreate great characteristics depth details as well as fill the absent depth principles from under the strong will observations. The depth details and characteristics of a surface's details are two descriptions of the same

scene, which however express powerful fundamental connections. After lining up by warping, the fundamental connections among the depth map and the characteristics of a surface's image can be utilized for information recovery [7]. Depth recovery is the important humanistic issue of computer eyesight. More techniques are grown that indicate this problem. Everyone has individual actions attached to the picture concept, obtaining method, performing arithmetic moment, and a lot. The difference of techniques is due to the non-uniqueness of the corresponding procedure added in-depth recovery from a pair of pictures [8]. Separating the depth details of a picture is to evaluate an interval among a gadget as well as a lens of the photographic equipment while capturing photos. This is important because it is divided into two categories: having movement and inactive depth, evaluating algorithm [9].

In machine view, many of the studies on recovering scene systems are situated on a pinhole camera model. The depth recovery approaches often model the image capture method on the premise that all depths inside a scene are in focal point at the same time, whereas the photometric detail shown by a pinhole camera ideal [10]. Thus, in this article, we present different features of the sports image decomposition issue utilizing the Moreau envelope as well as depth recovery. The major contribution of the paper is described below:

(i) The novelty of the paper is that Moreau envelope and depth recovery are the most effective techniques for sports image decomposition

(ii) The parameters recognition rate and accuracy are compared with various techniques

The rest of this article is structured as follows: Literature survey is given in the second section. The third section presents the proposed methodology. The fourth section exposed the result and discussion, and the fifth section expresses the conclusion.

2. Literature Survey

Yuanhui [11] combined the convolution neural network as well as probability map design to discover the decomposition method with great correctness as well as exact recognition rate and proposed a single-image intrinsic image decomposition technique that was on natural pictures as well as standard dataset pictures. The image intrinsic decomposition technique was oriented on depth convolutional neural networks as well as probabilistic graphical designs. Hui et al. [12] proposed various stage image decomposition techniques that were oriented on latent poor representation, which was known as MDLatLRR. The proposed decomposition design can be utilized a lot of picture transformation fields. The MDLatLRR-based fusion foundation was grown for fusing infrared as well as visible pictures. The results showed that the performance of the proposed technique was greater than that of methods that already exist.

Ling et al. [13] proposed a novel shadow removal algorithm that was oriented on multiscale picture decomposition that may regain the lighting for complicated shadows accompanying various surface equipment as well as inconsistent illumination. The information for the shadow-free coating image was recreated, as well as the most recent shadow ignorant result. The strength of the technique in indoor and outdoor complex situations was demonstrated. Selesnick [14] defined a generalisation of a certain nonvariable convex cost function that can produce multiple exact assessments of piecewise fixed signals. The recent cost function added a nonconvex penalty sketched to develop the convexity of the cost function. The projected full differentiation denoising techniques have to be executed utilizing forward-backward break-up.

According to Liu et al. [15], the flip starting approach is used to get a model's whole response-ability of the net confronting the human body and investigated the key steps as well as functions for trampoline somersaults, as well as the usage of artificial intelligence for performance recognition in health management and sports areas. The article's influence is demonstrated with exploratory outcomes and may simplify the procedure of identification of trampoline somersaults.Chen and Little [16] maintained a novel camera pose engine. It has three indicated free parameters so that it can powerfully operate many cameras that pose and match end images; educate compact deep features by way of a Siamese network from the paired-end image, camera pose, and creating a feature-pose database; and then use a novel two-GAN ideal to discover the field that is noticed in original images. This technique not only demonstrates rebutting on synthetic data, but it also achieves cutting-edge accuracy on a prominent soccer dataset and extremely good performance on a volleyball dataset.

Wenrui [17] analyzed the depth model technology's construction and optimization, and based on the deep network design, the migration learning technology is analyzed. The use of sports picture detection technology is analyzed by using sports video. To comprehend the acceptance of the sports method, combines image recognition and image processing technology. The findings of this study's sports picture detection technique suggest that it has some applicability. Xin [18] implemented a Messy Error Control Algorithm in the authentic reconstruction of approximate sports image capture specs for the complicated method. The manufacturing technique is utilized to express a three-dimensional dynamic simulation form of the human body while shifting. The messy control algorithm approach improved the genuineness of 3D dynamic simulation of human movement-picture categorization.

3. Proposed Methodology

This paper employs Moreau envelope and depth recovery for sports image decomposition. The application of the Moreau envelope in describing a non-separable nonconvex TV denoising penalty which develops the TV denoising cost movement's convexity was presented. The depth recovery work is to recreate great characteristics depth

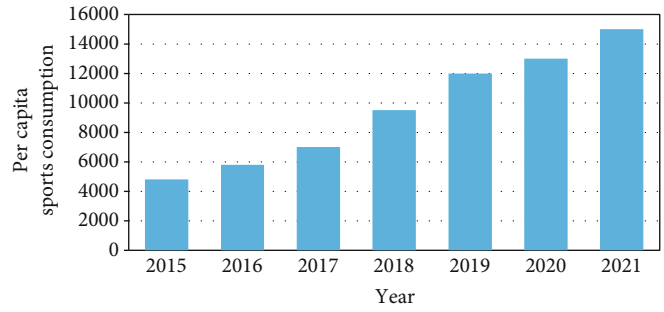

Figure 1: Nonconvex function analysis.

details as well as fill the absent depth principles from under the strong will observations. The mathematical expressions and the respective definitions based on the abovementioned methods are expressed in the coming sub-section.

3.1. Moreau Envelope. A way to smooth an arbitrary convex functional is the Moreau envelope, and it offers various benefits in optimization [19]. Optimization, nonlinear analysis, and signal recovery are all examples of applications. The Moreau envelope function and accompanying proximal mapping play an important role [20]. One of the important methods for constrained optimization is the Augmented Lagrangian Method [21]. In the convex analysis, there is a strong connection among lower half continuous convex movements and its Moreau envelope; this motivated many authors to investigate the Moreau envelope's properties of movements of a few divisions of nonconvex functions [14, 22, 23]. Researchers presented how the Moreau envelopes enable us to acquire the sub-differential resolutions for a lot of divisions of nonconvex functions [24–26]. Figure 1 shows the nonconvex function analysis.

Let us consider that the function $g \in \Theta_p(\psi)$ and the Moreau envelope $\delta_g : \psi \longrightarrow \nabla$ of g the index $\delta \in (0,\infty)$ are expressed as follows:

(i) Lower boundary $(\text{for } all\, \delta \in (0,\infty), \forall y \in \psi) g(y) \geq {}^{\delta}g(y)$

(ii) The pointwise convergence function ${}^{\delta}g$ based on the domain (g) as $\delta \longrightarrow 0$

$$\underset{\delta \downarrow 0}{LIM}\, {}^{\delta}g(y) = g(y)\ (\forall y \in domain(g)). \tag{1}$$

The bounded set $T \subset domain(g)$ is continuously uniformed in g and on T; the ${}^{\delta}g$ uniformly converges to g. Thus,

$$\underset{\delta \downarrow 0}{LIM}\ \underset{y \in t}{SUP} \left|{}^{\delta} g(y) - g(y)\right| = 0. \tag{2}$$

(iii) ${}^{\delta}g$ (Lipschitz continuity of Frechet derivative): $\mu \longrightarrow \nabla$ is the Frechet derivative, and it is denoted by

$$\diamond^{\delta} g(y) = \frac{y - PROX_{\delta g}(y)}{\delta} = \frac{y - (J + \delta \partial g)^{-1}(y)}{\delta}, \tag{3}$$

where $\diamond^{\delta} g(y)$ represents the Lipschitzian. The Moreau envelope with employed sciences is studied for absolute rate functions $|.|: \nabla \longrightarrow [0, \infty)$. The absolute rate function of the Moreau envelope is verified by

$${}^{\delta}|u| := \begin{cases} \dfrac{1}{2\delta} u^2, & \text{if } |u| \leq \delta \\ |u| - \dfrac{1}{2}\delta, & otherwise \end{cases}, \tag{4}$$

where δ denotes the scaling factor

$$q : \nabla \longrightarrow \nabla u \longrightarrow \begin{cases} \dfrac{1}{2} u^2, & \text{if } |u| \leq \delta \\ \delta |u| - \dfrac{1}{2}\delta^2, & otherwise \end{cases}. \tag{5}$$

The Huber's M cost function is utilized for evaluation problems:

$$FIND\, y^* \in ARG \underset{y \in \nabla^o}{MIN} \sum_{j=1}^{n} q\left(\left(B_y - c\right)_j\right), \tag{6}$$

where the underlying linear design is represented by $B \in \nabla^{n \times o}$, the data vector is denoted by $c \in \nabla^n$, and the parameter vector is represented by $y \in \nabla^o$. Usually, the computational problem has not been ever resolved; the proximity operator's efficiency is confirmed in the bounded dimensional scenario; then, $g \in \Theta_p(\nabla^o)$ is expressed in terms $g_j \in \Theta_p(\nabla)\ (j = 1, 2, \cdots \cdots, o)$ by

$$g : \nabla^o \longrightarrow \nabla : (y_1, \cdots, y_o) \mapsto \sum_{j=1}^{o} g_j\left(y_j\right) \tag{7}$$

$$PROX_{\delta g}(y_1, .. \cdots, y_o) = \left(PROX_{\delta g1}(y_1), .. \cdots \cdots, PROX_{\delta g o}(y_o)\right) \tag{8}$$

In this case, $PROX_{\delta g}(y_1, \cdots . \cdots, y_o)$ computation is decreased to find the $PROX_{\delta gj}(y_j)$ unique minimize for every univariate convex function is expressed as

$$g_j(.) + \frac{1}{2\delta}\left|y_j - .\right|^2 (j = 1, .. \cdots, o) \tag{9}$$

Proximity operators in closed-form expression. In this case, $g \in \Theta_p(\nabla)$ is expressed as

$$g : y \mapsto \begin{cases} -\ln(y) \text{ if } y > 0; \\ \infty \text{if } y \le 0, \end{cases} \text{ for } \delta \in (0,\infty), \tag{10}$$

$$PROX_{sg}(y) = \frac{1}{2}\left(y + \sqrt{y^2 + 4\delta}\right) \tag{11}$$

Let us consider that $\{g_l\}_{l=1}^{o}$ is the orthonormal base of ∇^o; thus, the standard of inner products is determined. Therefore, it can be

$$PROX_g(y) = \sum_{l=1}^{o} \left(PROX_{gl}(\langle y, f_l\rangle)\right) f_l(y \in \nabla^o) \tag{12}$$

$$g : \nabla^o \ni y \mapsto \sum_{l=1}^{o} x_l |\langle y, f_l\rangle| \in \nabla, \tag{13}$$

By reducing the non-smooth convex function in the Moreau envelope,

$$PROX_g(y) = \sum_{l=1}^{o} SGN(\langle y, f_l\rangle)\text{MAX}\{|\langle y, f_l\rangle| - x_l, 0\} f_l(y \in \nabla^o). \tag{14}$$

Remark 1. Proximity operator using Legendre –Fenchel Transform. Let us consider $\eta \in \Theta_p(\nabla^n), M \in \nabla^{n\times o}$ and $e \in INT(T)$, where

$$T : M(\nabla^o) - domain(\eta) \coloneqq \{My - z \in \nabla^n | y \in \nabla^o \text{and } z \in domain(\eta)\}, \tag{15}$$

where the interior T is represented by $INT(T)$. Determine $\eta^{\sim} \in \Theta_p(\nabla^o)$ through $\eta^{\sim} : y \mapsto \eta(My - e)$ and then the arbitrarily function fixed with $y \in \eta^o$ and $z \in (0,\infty)$:

$$\begin{aligned} PROX_{\delta\tilde{\eta}}(y) &\coloneqq ARG\underset{a\in\nabla^o}{\text{MIN}}\left(\eta(a) + \frac{\tilde{1}}{2\delta}\|y - a\|^2\right) \\ &= ARG\underset{a\in\nabla^n}{\text{MIN}}\left(\eta(Ma - e) + \frac{1}{2\delta}\|y - a\|^2\right) \end{aligned} \tag{16}$$

$$\bar{z} \in ARG\underset{z\in\nabla^n}{\text{MIN}}\left(\eta^*(z) + \langle e, z\rangle + \frac{1}{2\delta}\|\delta M^u z - y\|^2\right) \tag{17}$$

$$PROX_{\nabla\tilde{\eta}}(y) = y - \delta M^u \bar{z} \tag{18}$$

where the transpose matrix M is denoted by $M^u \in \nabla^{o\times n}$ and the Legendre –Fenchel η^* is the conjugate of η. The Fenchel-type duality scheme is applied, and it is expressed as

$$\begin{aligned} -M^* z \_ \in \partial\vartheta\left(PROX_{\delta\eta\sim}(Y)\right)^{-} &= \left\{\nabla\nu\left(PROX_{\delta\eta\sim}(y)\right)\right\} \\ &= \left\{\frac{1}{\delta}\left(PROX_{\delta\eta\sim}(y)y\right)\right\}, \end{aligned} \tag{19}$$

$$\bar{z} \in ARG\underset{z\in\nabla^n}{\text{MAX}}\{\langle -e, z\rangle - \eta^*(z) - \vartheta^*(-M^u z)\} \tag{20}$$

$$= ARG\underset{z\in\nabla^n}{\text{MIN}}\left\{\vartheta^*(z) + \langle e, z\rangle + \frac{1}{2\delta}\left(\|-\delta M^u z + y\|^2 - \|y\|^2\right)\right\} \tag{21}$$

3.2. Depth Observation Model. Let $\bar{x}$ as well as x indicate the vector structure of the great quality fundamental truth depth map as well as the decreased one. The relation among $\bar{x}$ and x is described as

$$x = M\bar{x} + s, \tag{22}$$

From Equation (22), the term M indicates the observation matrix, as well as the additive white Gaussian type, and is denoted by s. Under various scenarios, various degradations can display as a mixture kind in the taken depth map and may be indicated by the observation matrix M.

3.2.1. Depth Representation Model. The mathematical formula to derive the depth representation model is stated in

$$x = M(a + c) + s, \tag{23}$$

From Equation (2), the term a signifies the decomposed piece-wise element, and the term c signifies the polynomial element.

$$E_y(a) = \sum_l \varphi_l(F_l a) \tag{24}$$

From Equation (24), the filtering matrix developed from a certain filtering operator is defined by F_l and φ_l: $Rn \longrightarrow R$ is the signal before controlling the sparsity of a in a few transformation domains:

$$E_z(c) = \frac{\delta}{2}\|z - Kt\|_2^2 \tag{25}$$

From Equation (25), the notation δ represents a weighting parameter, the Vander monde matrix is defined by K, and the polynomial coefficient's vector is indicated by t. For example, if $z = (z_1, z_2 \ldots z_S)^T$ is an S-dimensional vector, then

$$K = \begin{bmatrix} 1 & 2 & \cdots & 1 \\ 1 & 2 & \cdots & 2^d \\ 1 & 3 & \cdots & 3^d \\ \vdots & \vdots & \ddots & \vdots \\ 1 & S & \cdots & S^d \end{bmatrix} t = \begin{bmatrix} t_0 \\ t_1 \\ \vdots \\ t_d \end{bmatrix}. \tag{26}$$

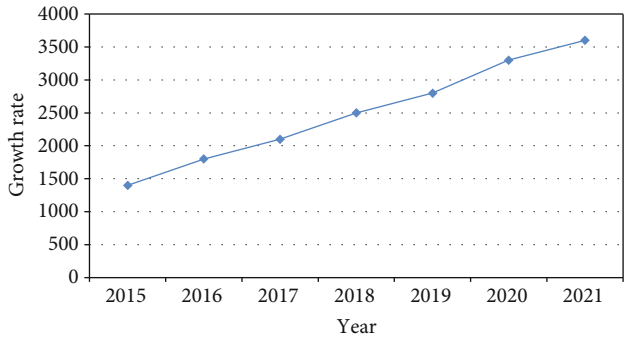

Figure 2: Comparative analysis of recognition rate.

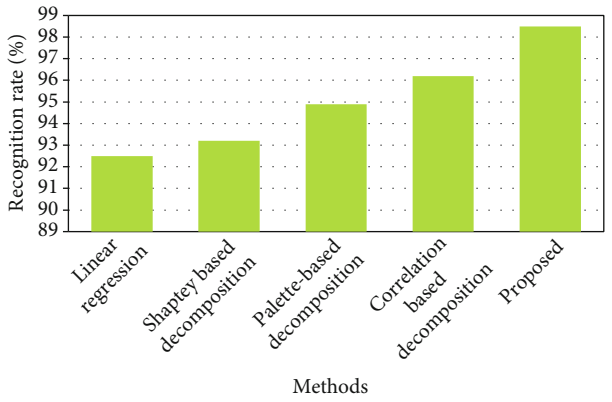

Figure 3: Accuracy calculation.

The degree of polynomial factor is denoted as d. The polynomial approximation's second order is called $d = 2$ and is enough to support the polynomial element of the depth patch.

4. Result and Discussion

In this section, the recognition rate, growth rate, and per capita sports consumption rate were evaluated and described below. Figure 2 shows the comparative analysis of the recognition rate of the proposed method. Here, the x-axis specifies various methods, and the y-axis specifies the regression rate. The recognition rate is higher for the proposed method compared to other methods. This proposed design is distinguished with existing techniques like linear regression, sharply based decomposition, palette-based decomposition, and correlation-based decomposition.

Figure 3 represents the accuracy calculation of three different qualities of the image. Three sets of images used for the analysis are low, medium, and high-quality images. The low quality, medium-quality, and high-quality images have a lower accuracy rate when no algorithm is used. For all three qualities, the accuracy rate is higher when the proposed method is applied. Figure 4 denotes x-axis as years and y-axis as per capita sports consumption. Every year, per capita sports consumption is calculated, and the survey is conducted from 2016 to 2021. From this bar graph, the year 2021 has a high range of per capita sports consumption, and the year 2016 has a low range of per capita sports consumption. The graph shows a rapid increment of per capita sports consumption year by year. Figure 5 represents a growth rate of every year and the X; the y-axis is the year and growth rate, respectively. The survey is conducted from

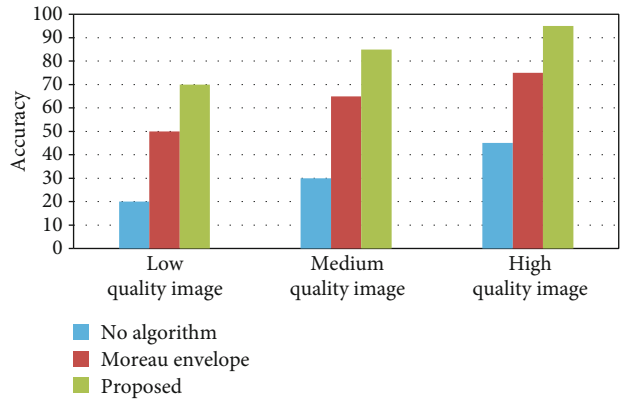

Figure 4: Analysis of per capita sports consumption growth.

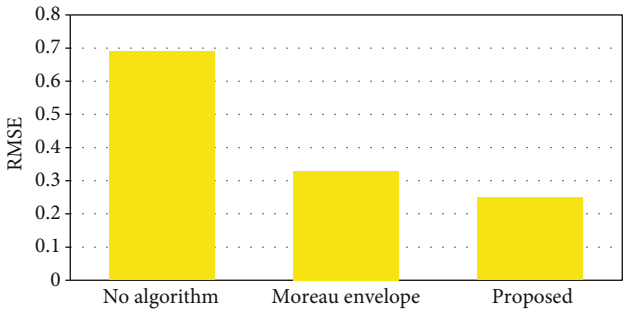

Figure 5: Growth rate of domestic sports events.

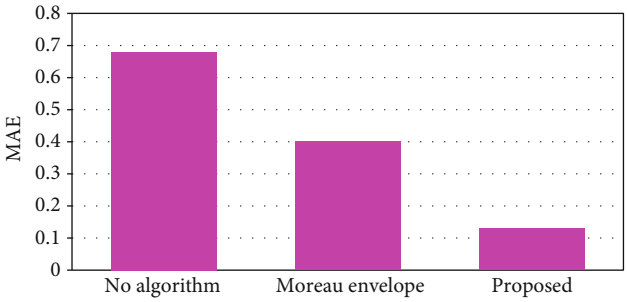

Figure 6: Root mean square error analysis.

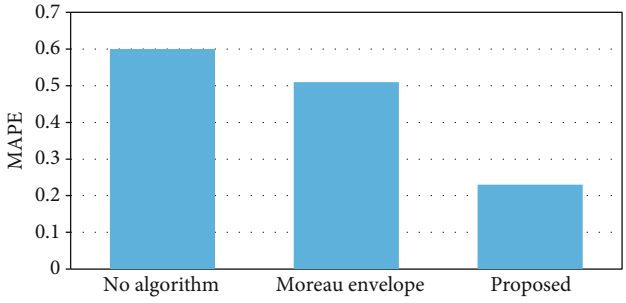

Figure 7: Mean absolute error analysis.

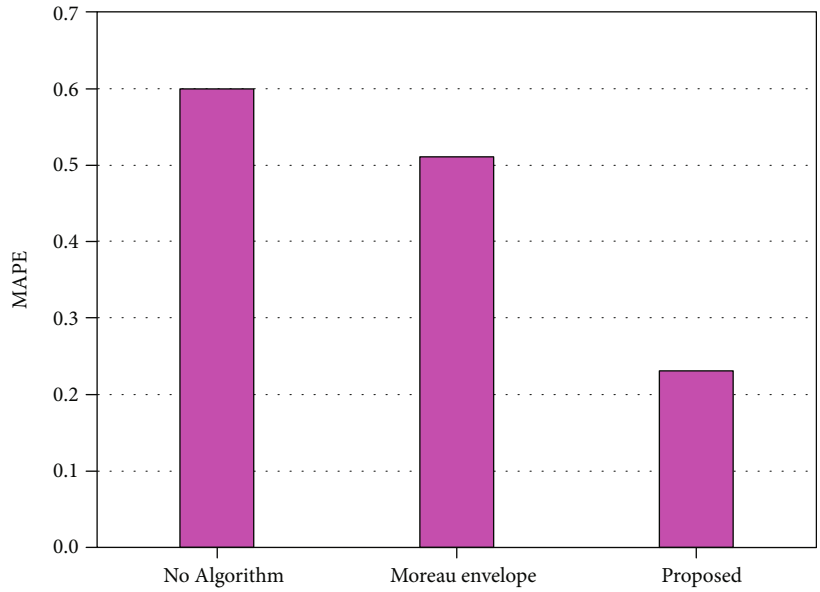

Figure 8: Comparison of mean absolute percentage error.

2016 to 2021 for determining the growth rate. From this survey, the year 2021 shows an enormous growth rate, and the year 2016 shows a very low growth rate. The graph shows a rapid growth rate from the year 2016 to 2021. Figure 6 describes a graphical representation of the root mean square error. An analysis was conducted by applying the no algorithm, Moreau envelope, and proposed method. The x-axis denotes the various methods applied. The y-axis denotes the root mean square error value. The graph shows that the root mean square error value of the proposed technique is low when distinguished from the various techniques.

Figure 7 depicts a graphical representation of the mean absolute error. The values of mean absolute error are denoted in y-axis. Various methods, no algorithm, Moreau envelope, and the proposed method are used for analysis, and they are denoted in the x-axis. The result revealed that the mean absolute error value of the proposed method is low while comparing with the other methods.

The graphical representation of mean absolute percentage error is depicted in Figure 8. The x-axis indicates the various methods applied for the analysis, and y-axis expresses the value of the mean absolute percentage error. As per the outcomes, the mean absolute percentage error value of the proposed approach is lower than the various techniques.

5. Conclusion

Sports image decomposition technology is worldly utilized in dissimilar fields, and the technologies of sports image action identification oriented on sports image transformation technologies may be apt. This paper expresses different aspects of the sports image decomposition issue utilizing the Moreau envelope as well as depth recovery. In the 1960s, the Moreau envelope $e_r f$ was expressed in its actual format by Jean- Jacques Moreau. A path to smooth an arbitrary convex function is the Moreau envelope, and it offers different advantages in optimization. In optimization, nonlinear analysis, as well as signal recovery Moreau envelope function, and associated proximal mapping play major parts. Depth recovery techniques often represent the sports image acquisition method by assuming that all depths in a scene are at the same focus point at the same time, whereas the picture via a pinhole camera model provides photometric information. It is dearth geometric information. The recognition rate, growth rate, and per capita sports consumption rate are measured and compared. Three sets of images are used for the analysis: low, medium, and high-quality images. For all three qualities, the accuracy rate is higher for this proposed technique. The proposed approach is compared with existing techniques such as linear regression, sharply based decomposition, palette-based decomposition, and correlation-based decomposition. The parameters of recognition rate and accuracy are compared with dissimilar techniques. While comparing other techniques, our proposed method is effective.

Data Availability

The data used to support the findings of this study are available from the corresponding author upon request.

Conflicts of Interest

The author declares that there is no conflict of interest.

References

[1] Y. Lucet, "What shape is your conjugate? A survey of computational convex analysis and its applications," *SIAM Review*, vol. 52, no. 3, pp. 505–542, 2010.

[2] V. Roulet and Z. Harchaoui, "Differentiable Programming á la Moreau," 2020, https://arxiv.org/pdf/2012.15458.pdf.

[3] W. Hare and C. Sagastizábal, "Computing proximal points of nonconvex functions," *Mathematical Programming*, vol. 116, no. 1-2, pp. 221–258, 2009.

[4] J. F. Aujol, G. Gilboa, T. Chan, and S. Osher, "Structure-texture image decomposition—modeling, algorithms, and parameter selection," *International Journal of Computer Vision*, vol. 67, no. 1, pp. 111–136, 2006.

[5] M. J. Fadili, J. L. Starck, J. Bobin, and Y. Moudden, "Image decomposition and separation using sparse representations: an overview," *Proceedings of the IEEE*, vol. 98, no. 6, pp. 983–994, 2009.

[6] T. L. Hwang, J. J. Clark, and A. L. Yuille, "A depth recovery algorithm using defocus information," in *1989 IEEE Computer Society Conference on Computer Vision and Pattern Recognition*, pp. 476-477, San Diego, CA, USA, 1989.

[7] J. Yang, X. Ye, and P. Frossard, "Global auto-regressive depth recovery via iterative non-local filtering," *IEEE Transactions on Broadcasting*, vol. 65, no. 1, pp. 123–137, 2018.

[8] B. Cyganek, "Depth recovery with an area based version of the stereo matching method with scale-space tensor representation of local neighborhoods," in *International Conference on Computational Science*, pp. 548–551, Kraków, Poland, 2004.

[9] H. Akbarally and L. Kleeman, "3D robot sensing from sonar and vision," in *Proceedings of IEEE international conference on robotics and automation*, pp. 686–691, Minneapolis, MN, USA, 1996.

[10] S. Chaudhuri and A. N. Rajagopalan, "Depth recovery from defocused images," in *Depth from defocus: a real aperture imaging approach*, Springer, New York, NY, 1999.

[11] Y. Yu, "Intrinsic decomposition method combining deep convolutional neural network and probability graph model," *Computational Intelligence and Neuroscience*, vol. 2022, 11 pages, 2022.

[12] H. Li, X. J. Wu, and J. Kittler, "MDLatLRR: a novel decomposition method for infrared and visible image fusion," *IEEE Transactions on Image Processing*, vol. 29, pp. 4733–4746, 2020.

[13] L. Zhang, Q. Yan, Y. Zhu, X. Zhang, and C. Xiao, "Effective shadow removal via multi-scale image decomposition," *The Visual Computer*, vol. 35, no. 6-8, pp. 1091–1104, 2019.

[14] I. Selesnick, "Total variation denoising via the Moreau envelope," *IEEE Signal Processing Letters*, vol. 24, no. 2, pp. 216–220, 2017.

[15] Y. Liu, H. Dong, and L. Wang, "Trampoline Motion Decomposition Method Based on Deep Learning Image Recognition," *Scientific Programming*, vol. 2021, Article ID 1215065, 8 pages, 2021.

[16] J. Chen and J. J. Little, "Sports camera calibration via synthetic data," in *Proceedings of the IEEE/CVF conference on computer vision and pattern recognition workshops*, Long Beach, CA, USA, 2019.

[17] W. Yang, "Analysis of sports image detection technology based on machine learning," *EURASIP Journal on Image and Video Processing*, vol. 2019, no. 1, 8 pages, 2019.

[18] X. Xu, L. Li, and A. Sharma, "Controlling messy errors in virtual reconstruction of random sports image capture points for complex systems," *International Journal of System Assurance Engineering and Management*, pp. 1–8, 2021.

[19] C. Planiden and X. Wang, "Proximal mappings and Moreau envelopes of single-variable convex piecewise cubic functions and multivariable gauge functions," in *Nonsmooth optimization and its applications*, Birkhäuser, Cham, 2019.

[20] C. Kan and W. Song, "The Moreau envelope function and proximal mapping in the sense of the Bregman distance," *Nonlinear Analysis: Theory, Methods & Applications*, vol. 75, no. 3, pp. 1385–1399, 2012.

[21] J. Zeng, W. Yin, and D. X. Zhou, "Moreau envelope augmented Lagrangian method for nonconvex optimization with linear constraints," 2021, https://arxiv.org/abs/2101.08519.

[22] I. Kecis and L. Thibault, "Moreau envelopes of s-lower regular functions," *Nonlinear Analysis: Theory, Methods & Applications*, vol. 127, pp. 157–181, 2015.

[23] Z. Song, W. Huang, Y. Liao et al., "Sparse representation based on generalized smooth logarithm regularization for bearing fault diagnosis," *Measurement Science and Technology*, vol. 32, no. 10, article 105003, 2021.

[24] B. Grimmer, H. Lu, P. Worah, and V. Mirrokni, "The landscape of the proximal point method for nonconvex-nonconcave minimax optimization," 2020, https://arxiv.org/abs/2006.08667.

[25] A. Jourani, L. Thibault, and D. Zagrodny, "Differential properties of the Moreau envelope," *Journal of Functional Analysis*, vol. 266, no. 3, pp. 1185–1237, 2014.

[26] I. Yamada, M. Yukawa, and M. Yamagishi, "Minimizing the Moreau envelope of nonsmooth convex functions over the fixed point set of certain quasi-nonexpansive mappings," in *Fixed-point algorithms for inverse problems in science and engineering*, Springer, New York, NY, 2011.